SCIENCE CHINA
Chemistry

•ARTICLES•

April 2024 Vol.67 No.4: 1270–1276
https://doi.org/10.1007/s11426-023-1894-1

Highly efficient through-space charge transfer TADF molecule employed in TADF- and TADF-sensitized organic light-emitting diodes

Jiasen Zhang[1,2†], Deli Li[3†], Wei Li[1,2*], Yujie Wu[1,2], Xilin Mu[1,2], Chunyu Liu[1,2], Kaibo Fang[1,2] & Ziyi Ge[1,2*]

[1]*Zhejiang Provincial Engineering Research Center of Energy Optoelectronic Materials and Devices, Ningbo Institute of Materials Technology and Engineering, Chinese Academy of Sciences, Ningbo 315201, China;*
[2]*Center of Materials Science and Optoelectronics Engineering, University of Chinese Academy of Sciences, Beijing 100049, China;*
[3]*State Key Laboratory of Luminescent Materials and Devices and Institute of Polymer Optoelectronic Materials and Devices, South China University of Technology, Guangzhou 510640, China*

Received October 27, 2023; accepted December 6, 2023; published online January 8, 2024

The inception and harnessing of excitons are paramount for the electroluminescence performance of organic light-emitting devices (OLEDs). Through-space charge transfer (TSCT) *via* intramolecular interaction has proved to be one of the most potent techniques employed to achieve 100% internal quantum efficiency. However, molecular strategies utilized to comprehensively enhance the electroluminescent performance of TSCT emitters regarding improving the photoluminescence quantum yield (PLQY) and elevating the light out-coupling efficiency remain arduous. To surmount this challenge, we deliberately designed and synthesized a proof-of-concept TSCT emitter called CzO-TRZ by incorporating an extra carbazole donor into spiro-heterocyclic architecture. The introduction of rigid spiral fragments can immensely boost the horizontal orientation dipole ratio and establish an extra through-bond charge transfer (TBCT) radiative decay channel. As a result, a very high PLQY of 98.7%, fast k_{RISC} of 2.2×10^5 s^{-1} and high k_r^s of 2.2×10^7 s^{-1}, and an ultrahigh horizontal dipolar ratio of 90% were concurrently achieved for CzO-TRZ blended films. Furthermore, corresponding thermally activated delayed fluorescence (TADF)- and TADF-sensitized fluorescence (TSF)-OLEDs based on CzO-TRZ demonstrated external quantum efficiencies (EQEs) of 33.4% and 30.3%, respectively, highlighting its versatile applications as both an emitter and sensitized host.

organic electronics, organic light-emitting diodes, polycyclic aromatic hydrocarbons, multiple-resonance

Citation: Zhang J, Li D, Li W, Wu Y, Mu X, Liu C, Fang K, Ge Z. Highly efficient through-space charge transfer TADF molecule employed in TADF- and TADF-sensitized organic light-emitting diodes. *Sci China Chem*, 2024, 67: 1270–1276, https://doi.org/10.1007/s11426-023-1894-1

1 Introduction

Equipped with virtues of low power consumption, rapid response, broad color range, wide viewing angles, and flexibility, organic light-emitting diodes (OLEDs) have ascended to the apex of cutting-edge technology in the realm of flat-panel displays and solid-state lighting [1–8]. A fundamental prerequisite for efficient OLED emitters lies in their proficiency in harnessing all the excitons generated under electrical excitation. Through-space charge transfer (TSCT)-based thermally activated delayed fluorescence (TADF) emitters feature minimal overlaps of frontier molecular orbitals, resulting in highly efficient reverse intersystem crossing (RISC) processes [9–11]. This allows for the almost complete utilization of electrical excitons, leading to a sig-

†These authors contributed equally to this work.
*Corresponding authors (email: liwei1987@nimte.ac.cn; geziyi@nimte.ac.cn)

nificant increase in the electroluminescence (EL) efficiency of OLEDs [12,13].

To create effective TSCT-TADF emitters, two electron-rich and electron-poor π units are needed close enough to form spatial intramolecular noncovalent interaction within the molecular systems [14–18]. With this conceptual mechanism, lots of TSCT-TADF emitters have been created. In 2020, Liao *et al*. [19] reported that a TSCT-type emitter, DMB, *via* a rigid linker and sky-blue OLEDs employing DM-B achieved a peak external quantum efficiency (EQE) of 27.4%. Later that year, by rational modulation of the molecular geometry and donor-acceptor (D-A) distance to restrict the molecular conrotatory motion, as high as 30.8% EQE with a very flat efficiency roll-off of 7% at 1,000 cd m^{-2} was achieved by using TSCT molecule 2tDMG as the emitter in evaporation-processed OLEDs [20]. Although dozens of molecules with TSCT mechanisms have been discovered, their relatively low EL performances are evident, with EQEs hovering at approximately 10% to 20% [21–23]. This figure is still significantly lower than that of OLEDs utilizing conventional TADF emitters of the through-bond charge transfer (TBCT) type or those incorporating noble metal-containing phosphorescent emitters. The inferior EL efficiency of such emitters-based OLEDs can be attributed to their relatively lower photoluminescence quantum efficiencies (PLQEs) and radiative decay rate [24–26].

On the flip side, traditional TBCT-TADF materials, which typically have lifetimes lasting for microseconds or even milliseconds, are prone to aggregation concentration quenching (ACQ) due to electron-exchange interactions controlled by a Dexter energy transfer mechanism [27–30]. Employing a twisted molecular backbone with "inert" chemically isolated fragments can effectively enhance the PL and EL performance in traditional TADF emitters, thanks to the short-range nature of electron-exchange interactions. However, the concentration quenching mechanism of special TSCT-TADF emitters has yet to be explored, let alone the molecular design strategy that restricts such concentration quenching [31,32]. These long-standing and unresolved issues hinder further improving the EL performance of TSCT-TADF emitters. Therefore, creating TSCT-TADF emitters that can match the efficiency of conventional TBCT-TADF materials remains a formidable challenge, and finding comprehensive molecular strategies to enhance EL performance is imperative.

Crucially, the molecular orientation of emitting materials should be taken into consideration since it has a significant effect on the optical out-coupling efficiency (η_{out}) [33–36]. The previous document reports have revealed that the aspect ratio of the emitter, glass-transition temperature (T_g), and molecular weight are identified as key parameters for boosting the horizontal orientation dipole ratio [37–40]. Therefore, using a linear and planar molecular backbone, as well as increasing molecular weight, have become common approaches for the realization of high horizontal orientation for emitters [41]. Thus, strategies are needed to explore TSCT emitters since they usually have a specific molecular skeleton [42–44].

To deal with the dilemma, a proof-of-the-concept TSCT emitter, 10-(4-(4,6-diphenyl-1,3,5-triazin-2-yl)phenyl)-2′-(9-phenyl-9*H*-carbazol-3-yl)-10*H* spiro[acridine-9,9′-xanthene] (CzO-TRZ), *via* introducing an extra carbazole donor to spiro-heterocyclic architecture, was purposefully designed and synthesized (Figure 1a). Interestingly, in optimized geometry in the ground (S_0) state, the 9-phenyl-9*H*-carbazole (PhCz) donor is tilted faced to the acceptor 2,4,6-triphenyl-1,3,5-triazine (TRZ) and resulting in a unique "U" shaped molecular architecture (Figure 1c, d). The isosurfaces and scatter diagrams of the reduced density gradient (RDG) clearly illustrate the successful formation of the TSCT radiative decay channel (Figure 1b–d). To enhance the horizontal orientation dipole ratio, we also purposefully introduced a rigid spiral fragment and coupled it with the TRZ unit to form an extra TBCT radiative decay channel. A creative approach to molecule design can significantly improve the horizontal orientation dipole ratio in addition to increasing the radiative decay rate (k_r^s). X-ray crystallographic analysis unveiled an intermolecular acceptor-acceptor (A-A) π-π stacking. Instead of increasing the non-radiative attenuation rate, such A-A-type π-π stacking serves to rigidify the molecular backbone. In fact, simulation of the monomer, dimer, and trimer of the CzO-TRZ crystal clearly indicated that the inter- and intramolecular transitions dominated the energy transfer processes, thereby preventing long-range energy transfer. Consequently, a very high PLQY of 98.7%, fast k_{RISC} of 2.2×10^5 s^{-1} and high k_r^s of 2.2×10^7 s^{-1}, and an ultra-high horizontal dipolar ratio of 90% were concurrently achieved for CzO-TRZ blended films, suggesting tremendous potential in OLED applications. In accompany with many advantages, the corresponding TADF- and TADF-sensitized fluorescence (TSF)-OLEDs achieved 33.4% and 30.3% external quantum efficiencies (EQEs), verifying their versatile applications both as emitter and sensitized host.

2 Results and discussion

The synthetic procedures of CzO-TRZ are summarized in Supporting Information online. The thermogravimetric (TGA) and differential scanning calorimetry (DSC) analysis curves indicated excellent thermal and morphological stabilities (Figure S1 and Table S1, Supporting Information online), suitable for vacuum deposition of device fabrication. The S_0 state of CzO-TRZ was initially investigated by den-

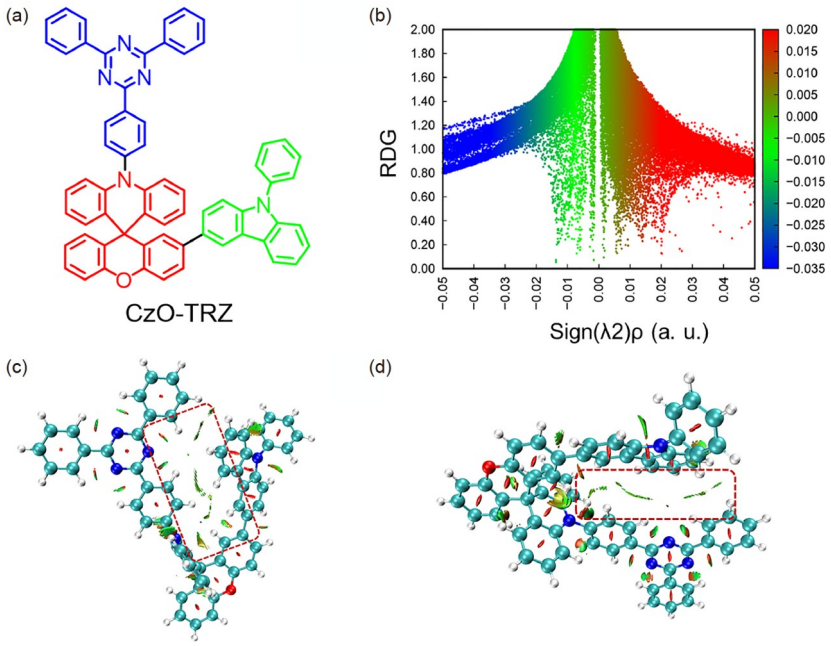

Figure 1 (a) Chemical structure of **CzO-TRZ**; (b–d) reduced density gradient (RDG) isosurfaces and scatter diagrams of **CzO-TRZ** (color online).

sity functional theory (DFT) calculation at the B3LYP/6-31G* level. A tilted face-to-face alignment of PhCz and TRZ acceptor (TSCT radiative decay channel) and a crooked spiral donor-π-TRZ acceptor (TBCT radiative decay channel) were visualized. The highest occupied molecular orbital (HOMO) was located on the PhCz unit and the adjacent benzene fragment, while the lowest unoccupied molecular orbital (LUMO) was mainly on the TRZ acceptor, verifying the formation of the TSCT transfer channel in CzO-TRZ (Figure S2). Based on the optimized S_0 geometry, the RDG analysis of CzO-TRZ was implemented (Figure 1b–d). The isosurface is colored on a blue-green-red scale based on sign $(\lambda_2)\rho$ with a range from −0.05 to 0.05. The red region denotes the repulsive effect. Meanwhile, the blue region represents the strong attractive interaction. A large area of the green region (red dashed circles) located between PhCz and TRZ unit, illustrating relatively strong π-π interaction and narrow spatial donor-acceptor distance (in a range of 3.2 to 3.5 Å), in favor of forming intramolecular π···π interactions and facilitating the electronic transition *via* TSCT process.

The insights on understanding the intermolecular interaction and stacking tendency may disclose the mysteries of the concentration quenching mechanism of the TSCT-TADF emitters. Therefore, single crystals were grown from a mixture of methanol and chloroform by slow vapor-liquid diffusion method (CCDC number: 2254430) (Figure 2 and Figure S3, Table S2). X-ray crystallographic analysis revealed a head-to-tail packing mode with a small interlayer slide adjacent (Figure 2), suggesting a J-aggregate was formed. The CzO-TRZ crystal shows a monoclinic system with *P*-1 space group and crystal cell parameters of a=9.0789 Å, b=9.1464 Å, c=30.349 Å, $\alpha = 82.5°$, $\beta = 81.6°$, $\gamma = 75.8°$ (Table S2). The intermolecular C–H···π and π-π interaction coexist in the CzO-TRZ crystal. Generally, it is believed that intermolecular π-π interaction might lead to serious ACQ, weakening emissive properties. However, a further high PLQY of 86.3% was revealed for CzO-TRZ crystal. Thus, the discovery of intermolecular π-π interaction in this molecule might benefit from rigidifying the molecular backbone and restricting the non-radiative decay rather than harming the emissive properties. The underlying reason could be due to the triplet exciton diffusion mechanism, which was induced by the DET mechanism and can be considered a double charge transfer process. In other words, both intermolecular π-π occurred in A-A and donor-donor (D-D), which can significantly lengthen the long-lived triplet exciton diffusion length. To gain a deeper understanding of the excited-state electronic structures, the chemical structures of the monomer, dimer, and trimer of CzO-TRZ were extracted for simulation (Figure 3), for the $S_0 \rightarrow S_1$ transition of the monomer, an intramolecular CT transition from the spiral donor to the TRZ unit was visualized. For the dimer, an additional transition from the spiral donor of one monomer to the TRZ unit of the adjacent monomer was revealed (Figure 3). Simulation of the trimer indicated that the intermolecular transition could hardly step over a monomer, suggesting the inter-and intramolecular transition dominated the energy transfer processes, which are in line with the description of the solely intermolecular A-A π-π interaction.

The UV-vis and PL spectra measured in toluene solution

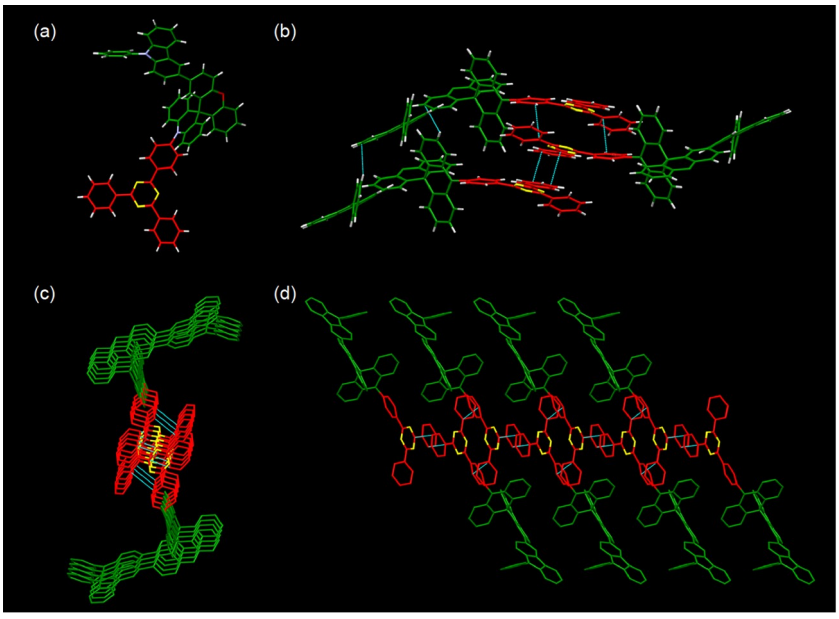

Figure 2 (a) The monomer and (b–d) molecular packing of CzO-TRZ single crystal (color online).

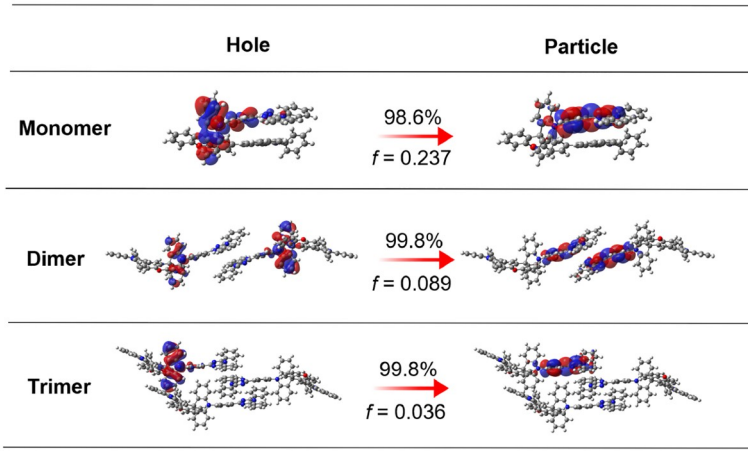

Figure 3 Natural transition orbits (NTOs) of monomer, dimer, and trimer chemical structures of CzO-TRZ calculated at M062X/6-31G* level. The corresponding transition energies and oscillator strength (*f*) values of CzO-TRZ were also provided for comparison (color online).

were investigated to verify the above research results (Figure 4a and Figure S5). The absorption band around 400 nm may arise from the combination of TSCT and TBCT transition. In PL spectra, a broad, structureless sky-blue emission peaking at 478 nm was recorded for CzO-TRZ (Figure 4a and Table S1). The low-temperature fluorescence and phosphorescence spectra have proceeded at 77 K in dilute toluene solution to ascertain the energy levels of S_1 and T_1 states. As expected, CzO-TRZ demonstrated a very small ΔE_{ST} of 33 meV (Figure 4a and Table S1). Time-transient PL spectrum and PLQY value of CzO-TRZ in a doped film were conducted in a nitrogen atmosphere to explore the PL property further (Figure S5). Impressively, a high PLQY of up to 98.7% is achieved for CzO-TRZ doped film. More importantly, high k_r^s of ~2.4×10^7 s^{-1} and k_{RISC} of ~3.3×10^5 s^{-1} were simultaneously achieved for CzO-TRZ doped film (Table S3). The values of k_r^s and k_{RISC} are all much higher than that of the reported TSCT-TADF molecules. On the other hand, PLQY and horizontal dipole orientation factor are the two most important essential parameters that determine EL performance. Hence, to precisely assess the optical out-coupling property and EL performance of these compounds, variable-angle PL measurement of the 20 wt% doped film in dibenzo[b,d]furan-2,8-diylbis(diphenylphosphine oxide) (PPF) was measured (Figure 4b). Noticeably, the horizontal dipole ratio of CzO-TRZ was attained 90%. Such a high horizontal dipole ratio can extremely enhance its EL performance.

To evaluate their EL performances, OLED was fabricated

with the device architecture of ITO/HATCN (10 nm)/TAPC (30 nm)/mCP (5 nm)/PPF: 20 wt% CzO-TRZ (30 nm)/PPF (5 nm)/TmPyPb (50 nm)/ LiF (1 nm)/Al (120 nm) (Figure 5a, b). Where HATCN, TAPC, mCP, and TmPyPb served as hole-injection, hole-transport, electron-blocking, and electron-transport materials, respectively. Especially, PPF serves as host and hole-blocking material simultaneously. In emitting layer, the optimal doping concentration is 20 wt%. Noticeably, an as high as 33.4% EQE and power efficiency of 104 lm W^{-1} was achieved by CzO-TRZ-based sky-blue OLED, which is one of the highest EQEs of TSCT emitters-based OLEDs (Figure 5c, d, Table S4).

Consider that high-definition (HD) display technology requires EL spectra with narrow full width at half-maximum (FWHM). Thus, CzO-TRZ was also used as a sensitizer in TSF-OLED. One multi-resonance (MR)-TADF compound BTC-BNCz was treated as an emitter [12], and the architecture of TSF-OLED of ITO/ HAT-CN (10nm)/TAPC (30nm)/mCP (10 nm)/ 1 wt% MR-TADF:20 wt% CzO-TRZ: PPF (30 nm)/ PPF (10 nm)/TmPyPb (40 nm)/ LiF (1 nm)/Al (150 nm) was fabricated (Figure 6). Greenish-blue emission with a peak of 496 nm and narrow full width at half-maximum (FWHM) of 39 nm were recorded, corresponding to CIE coordinate of (0.17, 0.53). TSF-OLED showed sig-

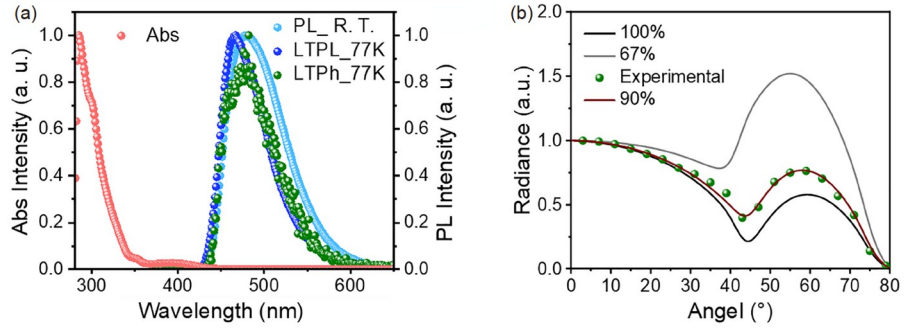

Figure 4 (a) UV-vis, room temperature PL, low-temperature PL (LTPL), and phosphorescent (LTPh) spectra in dilute toluene solution. (b) Measured p-polarized PL intensity of 20 wt% CzO-TRZ into PPF matrix as a function of the emission angle (color online).

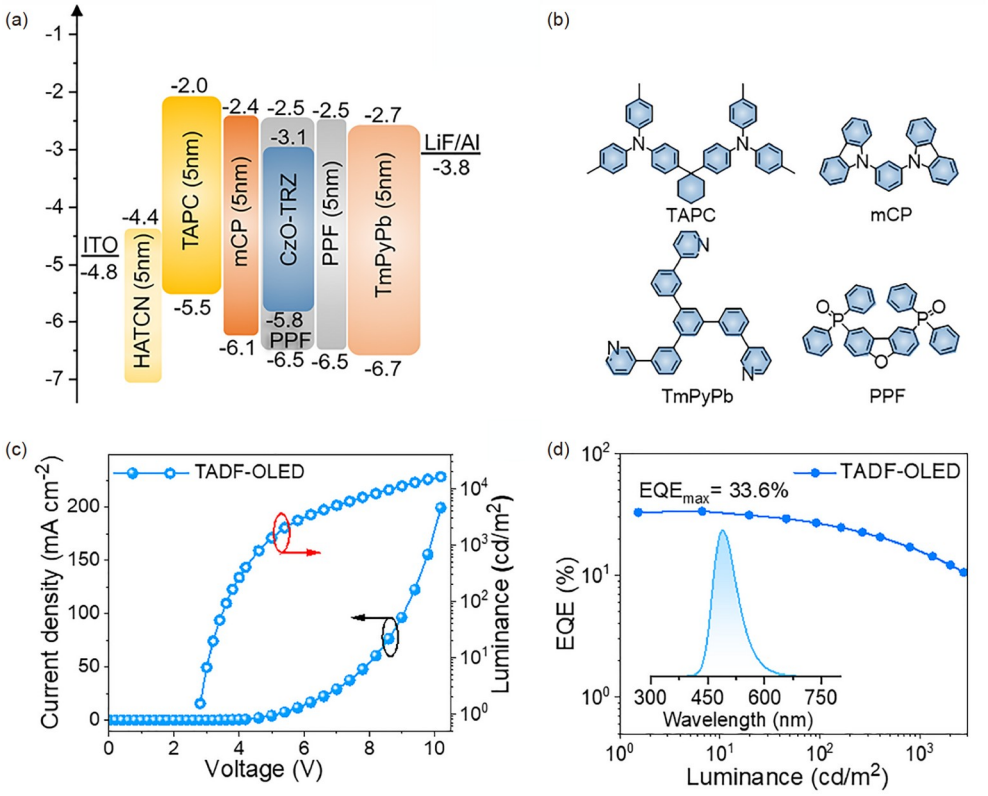

Figure 5 (a) Device architecture and energy diagram for CzO-TRZ based OLED. (b) Molecular structures of the relevant materials for device fabrication. (c) Current density-voltage-luminance curves. (d) EQE-luminance curve (inset: EL spectrum at 10 mA cm^{-2}) (color online).

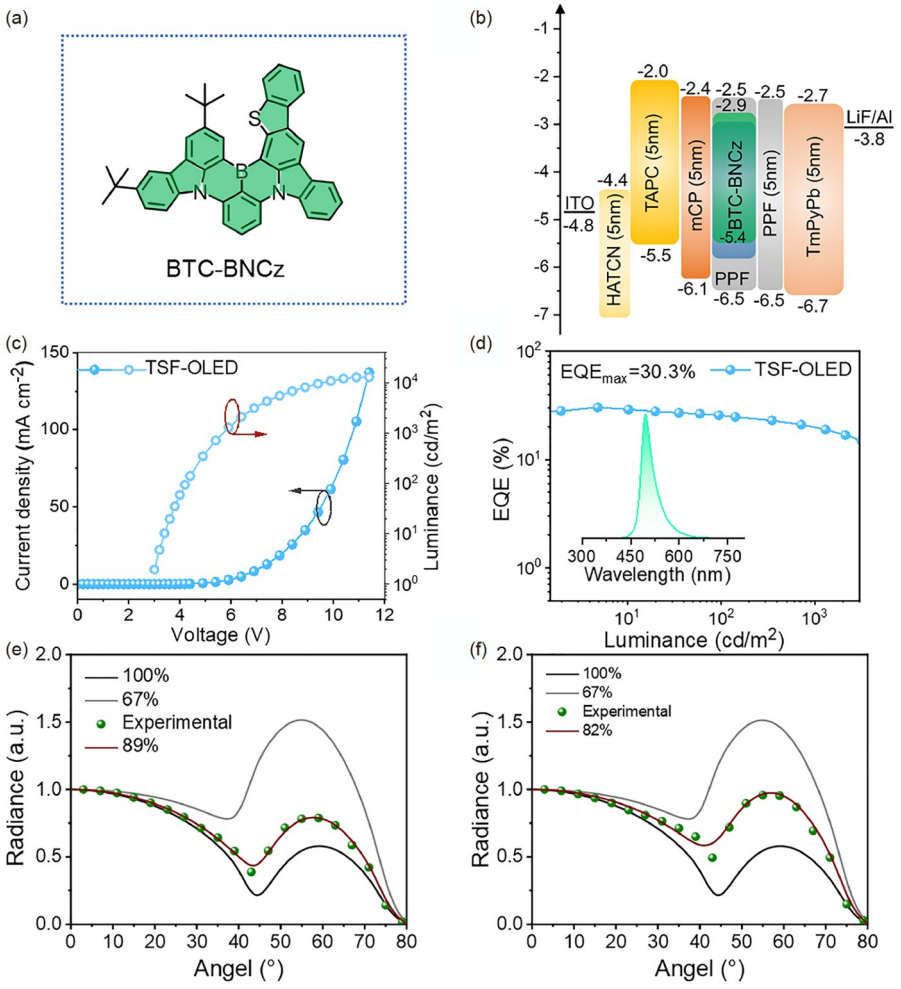

Figure 6 (a) Molecular structure of BTC-BNCz. (b) Device architecture and energy diagram for CzO-TRZ-based TSF-OLED; (c) current density-Voltage-Luminance curves; (d) EQE-Luminance curve (inset: EL spectrum at 10 mA cm^{-2}); (e) measured p-polarized PL intensity of 1 wt% BTC-BNCz:20 wt% CzO-TRZ into PPF matrix as a function of the emission angle; (f) measured p-polarized PL intensity of 1 wt% BTC-BNCz into PPF matrix as a function of the emission angle (color online).

nificantly high efficiency with a peak EQE of 30.3%. Moreover, the significant overlap between the PL spectrum of CzO-TRZ and the absorption spectrum of BTC-BNCz can lead to an efficient fluorescence resonanceenergy transfer (FRET) process in TSF-OLED (Figure S6). Additionally, the high EL performance of this TSF-OLED may also be attributed to the synergistic effect of the horizontally-aligned dipole orientation induced by CzO-TRZ on the transition dipole moment of BTC-BNCz. Precisely, the state-of-the-art EL performance of both TADF- and TSF-TADF OLEDs are achieved based on CzO-TRZ as emitter and sensitized host, ranking among TADF materials for achieving EQEs above 30% in both TADF- and TSF-OLEDs.

3 Conclusions

In summary, a versatile proof-of-concept emitter CzO-TRZ was purposefully designed and synthesized that incorporates both TSCT and TBCT transfer channels. X-ray crystallographic analysis revealed that the moderate intermolecular A-A type π-π interaction within this molecule is beneficial for rigidifying the molecular backbone and restricting the non-radiative decay rather than harming the emissive properties. Simulation of the trimer indicated that inter- and intramolecular transitions dominated the energy transfer processes and hindered long-range energy transfer. This led to the concurrent achievement of very high PLQY of 98.7%, fast k_{RISC} of 2.2×10^5 s^{-1}, high k_r^s of 2.2×10^7 s^{-1}, and the ultra-high horizontal dipolar ratio of 90% for CzO-TRZ blended films, highlighting its tremendous potential in OLED applications. Furthermore, TADF- and TSF-OLEDs achieved 33.4% and 30.3% EQEs, respectively, demonstrating their potential for high-performance optoelectronic devices and versatile applications as both an emitter and sensitized host. This article provides a feasible strategy and new insights into

boosting the EL performance of TSCT emitters with small efficiency roll-off, paving the way for practical applications in OLED technology and offering a multitude of advantages.

Acknowledgements This work was supported by the National Natural Science Foundation of China (U21A20331, 51773212, 81903743, 52003088), the Distinguished Young Scholars (21925506) and the Ningbo Key Scientific and Technological Project (2022Z124, 2022Z119).

Conflict of interest The authors declare no conflict of interest.

Supporting information The supporting information is available online at chem.scichina.com and link.springer.com/journal/11426. The supporting materials are published as submitted, without typesetting or editing. The responsibility for scientific accuracy and content remains entirely with the authors.

1 Tang CW, VanSlyke SA. *Appl Phys Lett*, 1987, 51: 913–915
2 Chao T, Lin Y, Yang C, Hung T , Chou H, Wu C, Wong K. *Adv Mater*, 2005, 17: 992–996
3 Zhang Q, Li J, Shizu K, Huang S, Hirata S, Miyazaki H, Adachi C. *J Am Chem Soc*, 2012, 134: 14706–14709
4 Yang Y, Cohn P, Eom SH, Abboud KA, Castellano RK, Xue J. *J Mater Chem C*, 2013, 1: 2867–2874
5 Hirata S, Sakai Y, Masui K, Tanaka H, Lee SY, Nomura H, Nakamura N, Yasumatsu M, Nakanotani H, Zhang Q, Shizu K, Miyazaki H, Adachi C. *Nat Mater*, 2015, 14: 330–336
6 Zhan L, Chen T, Zhong C, Cao X, Zhang Y, Zou Y, Bin Z, You J, Zhang D, Duan L, Yang C, Gong S. *Sci China Chem*, 2023, 66: 3213–3222
7 Ning W, Wang H, Gong S, Zhong C, Yang C. *Sci China Chem*, 2022, 65: 1715–1719
8 Zhang YP, Song SQ, Mao MX, Li CH, Zheng YX, Zuo JL. *Sci China Chem*, 2022, 65: 1347–1355
9 Cho TY, Lin CL, Wu CC. *Appl Phys Lett*, 2006, 88: 111106
10 Poitras D, Kuo CC, Py C. *Opt Express*, 2008, 16: 8003–8015
11 Jiang P, Miao J, Cao X, Xia H, Pan K, Hua T, Lv X, Huang Z, Zou Y, Yang C. *Adv Mater*, 2022, 34: e2106954
12 Park IS, Yang M, Shibata H, Amanokura N, Yasuda T. *Adv Mater*, 2022, 34: e2107951
13 Zhang Y, Li G, Wang L, Huang T, Wei J, Meng G, Wang X, Zeng X, Zhang D, Duan L. *Angew Chem Int Ed*, 2022, 61: e202202380
14 Kaji H, Suzuki H, Fukushima T, Shizu K, Suzuki K, Kubo S, Komino T, Oiwa H, Suzuki F, Wakamiya A, Murata Y, Adachi C. *Nat Commun*, 2015, 6: 8476
15 Hong X, Zhang D, Yin C, Wang Q, Zhang Y, Huang T, Wei J, Zeng X, Meng G, Wang X, Li G, Yang D, Ma D, Duan L. *Chem*, 2022, 8: 1705–1719
16 Chen Y, Zhang D, Zhang Y, Zeng X, Huang T, Liu Z, Li G, Duan L. *Adv Mater*, 2021, 33: e2103293
17 Nakanotani H, Higuchi T, Furukawa T, Masui K, Morimoto K, Numata M, Tanaka H, Sagara Y, Yasuda T, Adachi C. *Nat Commun*, 2014, 5: 4016
18 Wang S, Qiao M, Ye Z, Dou D, Chen M, Peng Y, Shi Y, Yang X, Cui L, Li J, Li C, Wei B, Wong WY. *iScience*, 2018, 9: 532–541
19 Tang X, Cui L, Li H, Gillett A, Auras F, Qu Y, Zhong C, Jones S, Jiang Z, Friend H, Liao L. *Nat Mater*, 2020, 19: 1332–1338
20 Wei J, Zhang C, Zhang D, Zhang Y, Liu Z, Li Z, Yu G, Duan L. *Angew Chem Int Ed*, 2021, 60: 12269–12273
21 Matsui K, Oda S, Yoshiura K, Nakajima K, Yasuda N, Hatakeyama T. *J Am Chem Soc*, 2018, 140: 1195–1198
22 Kondo Y, Yoshiura K, Kitera S, Nishi H, Oda S, Gotoh H, Sasada Y, Yanai M, Hatakeyama T. *Nat Photonics*, 2019, 13: 678–682
23 Oda S, Kawakami B, Kawasumi R, Okita R, Hatakeyama T. *Org Lett*, 2019, 21: 9311–9314
24 Zhang Y, Zhang D, Wei J, Liu Z, Lu Y, Duan L. *Angew Chem Int Ed*, 2019, 58: 16912–16917
25 Naveen KR, Lee H, Braveenth R, Karthik D, Yang KJ, Hwang SJ, Kwon JH. *Adv Funct Mater*, 2022, 32: 2110356
26 Yang M, Shikita S, Min H, Park IS, Shibata H, Amanokura N, Yasuda T. *Angew Chem Int Ed*, 2021, 60: 23142–23147
27 Zou Y, Hu J, Yu M, Miao J, Xie Z, Qiu Y, Cao X, Yang C. *Adv Mater*, 2022, 34: e2201442
28 Zhang Y, Zhang D, Huang T, Gillett AJ, Liu Y, Hu D, Cui L, Bin Z, Li G, Wei J, Duan L. *Angew Chem Int Ed*, 2021, 60: 20498–20503
29 Yang M, Park IS, Yasuda T. *J Am Chem Soc*, 2020, 142: 19468–19472
30 Han SH, Jeong JH, Yoo JW, Lee JY. *J Mater Chem C*, 2019, 7: 3082–3089
31 Meng G, Zhang D, Wei J, Zhang Y, Huang T, Liu Z, Yin C, Hong X, Wang X, Zeng X, Yang D, Ma D, Li G, Duan L. *Chem Sci*, 2022, 13: 5622–5630
32 Lee HL, Chung WJ, Lee JY. *Small*, 2020, 16: e1907569
33 Patil VV, Lee HL, Kim I, Lee KH, Chung WJ, Kim J, Park S, Choi H, Son W, Jeon SO, Lee JY. *Adv Sci*, 2021, 8: e2101137
34 Patil VV, Lim J, Lee JY. *ACS Appl Mater Interfaces*, 2021, 13: 14440–14446
35 Lee HL, Jeon SO, Kim I, Kim SC, Lim J, Kim J, Park S, Chwae J, Son W, Choi H, Lee JY. *Adv Mater*, 2022, 34: e2202464
36 Liu T, Cheng C, Lou W, Deng C, Liu J, Wang D, Tsuboi T, Zhang Q. *J Mater Chem C*, 2022, 10: 7799–7802
37 Luo M, Li W, Lyu L, Li D, Du S, Zhao M, Wang Z, Zhang J, Li Y, Ge Z. *Adv Opt Mater*, 2022, 11: 2202176
38 Zeng X, Wang X, Zhang Y, Meng G, Wei J, Liu Z, Jia X, Li G, Duan L, Zhang D. *Angew Chem Int Ed*, 2022, 61: e202117181
39 Taniguchi T, Itai Y, Nishii Y, Tohnai N, Miura M. *Chem Lett*, 2019, 48: 1160–1163
40 Burke K, Werschnik J, Gross EKU. *J Chem Phys*, 2005, 123: 62206
41 Runge E, Gross EKU. *Phys Rev Lett*, 1984, 52: 997–1000
42 Chen S, Xu H. *Chem Soc Rev*, 2021, 50: 8639–8668
43 Li D, Li M, Liu D, Yang J, Li W, Yang Z, Yuan H, Jiang S, Peng X, Yang G, Xie W, Qiu W, Gan Y, Liu K, Su S. *Adv Opt Mater*, 2023, 11: 2301084
44 Song X, Shen S, Zou S, Guo F, Wang Y, Gao S, Zhang Y. *Chem Eng J*, 2023, 467: 143557